



International Journal for Research Communications in Engineering, Emerging Technologies and Sciences (IJRCEETS)
Volume 1, Issue 2, November-2025

Cite: Dr. Santhi Sri Nerella, Dr. Sailaja C (2025), *Additive Manufacturing of Functionally Graded Materials for Aerospace Applications: A Comprehensive Review*, *International Journal for Research Communications in Engineering, Emerging Technologies and Sciences*, Vol. 01, issue (2), pp. 39-54.

Additive Manufacturing of Functionally Graded Materials for Aerospace Applications: A Comprehensive Review

Dr. Santhi Sri Nerella^{1*}, Dr. Sailaja C²

^{1*} Associate Professor, Matrusri Engineering College, Hyderabad, Telangana State, India

² Associate Professor, Dept. of Aeronautical Engineering, AMC Engineering College, Bangalore

Article info:

Article No.: IJRCEETSV11I20004

Submitted: 29/08/2025

Received in revised form: 17/10/2025

Accepted for publication: 26/10/2025

Available online: 14/11/2025

*Corresponding email:

sailajabcet@gmail.com



Abstract. Functionally Graded Materials (FGMs) represent a paradigm shift in structural material design, offering spatially tailored compositions and microstructures that eliminate sharp interface discontinuities found in traditional composites. This review comprehensively examines the state-of-the-art in additive manufacturing (AM) of FGMs for aerospace applications, covering process technologies including Selective Laser Melting (SLM), Directed Energy Deposition (DED), Binder Jetting (BJ), and Multi-material Extrusion (MME). We analyse the microstructural evolution, mechanical properties, thermal performance, and residual stress characteristics of AM-fabricated FGMs, with emphasis on material systems most relevant to aerospace: Ti-6Al-4 V/Inconel 718, Ti/ Al₂O₃, and Inconel/ W systems. Key findings reveal that DED enables continuous composition gradients with interlayer transition widths as narrow as 50–200 μm, achieving ultimate tensile strengths of 1050–1200 MPa in optimally processed FGM specimens. Computational design tools including Multiphysics FEA and topology optimization are reviewed alongside experimental validation datasets. Industrial case studies include turbine blade thermal barrier coatings, rocket nozzle liners, and hypersonic leading-edge components. Challenges in process qualification, non-destructive evaluation, and regulatory certification are discussed. Future research directions encompassing AI-guided process optimization, in situ monitoring, and sustainable AM feedstocks are identified.

Keywords: Functionally Graded Materials; Additive Manufacturing; Selective Laser Melting; Directed Energy Deposition; Aerospace Structures; Thermal Barrier Coatings; Ti-6Al-4 V; Inconel 718; Microstructure; Mechanical Properties

1. Introduction

The aerospace industry operates at the frontier of materials science, demanding components that simultaneously withstand extreme thermal gradients, high mechanical loads, oxidizing environments, and fatigue cycling while minimizing weight. Conventional engineering materials—even advanced titanium alloys, nickel superalloys, and ceramic composites—are fundamentally homogeneous and incapable of providing optimal performance across dramatically different operating conditions encountered within a single component, such as a turbine blade or re-entry vehicle nose cone. Functionally graded materials (FGMs) address this limitation through deliberate spatial variation in composition and/or microstructure, creating a gradient transition between two or more constituent phases. This concept was first introduced by Japanese researchers Koizumi and Niino in 1984 in the context of thermal barrier coatings for space-plane fuselages, where a sharp metal–ceramic interface causes catastrophic delamination under rapid thermal cycling. Since then, the field has expanded dramatically, driven in large part by the maturation of additive manufacturing (AM) technologies capable of depositing material layer by layer with programmable composition control.

Additive manufacturing, often termed 3D printing, has emerged as the enabling technology for FGMs because it naturally lends itself to spatially resolved material placement. Unlike subtractive or forming processes that operate on pre-existing bulk material, AM builds geometry from digital design files through sequential material deposition, enabling composition changes on a layer-by-layer, voxel-by-voxel, or continuous gradient basis. The synergy between the FGM design philosophy and AM process capabilities has opened a new frontier for aerospace structural components.

This review is organized as follows: Section 2 surveys FGM classification and material systems; Section 3 reviews AM process technologies and their FGM capabilities; Section 4 details microstructure and property outcomes; Section 5 covers computational design and simulation; Section 6 presents aerospace application case studies; Section 7 discusses challenges and future outlook; and Section 8 provides conclusions.

1.1 Motivation and Scope

The global aerospace AM market was valued at approximately USD 2.4 billion in 2023 and is projected to exceed USD 9.8 billion by 2032, reflecting a CAGR of 17.3%. In this context, metal AM for structural aerospace components represents the fastest-growing segment, with FGM-capable processes (DED and SLM) accounting for a growing share. This review specifically focuses on (i) metallic and metal-ceramic FGM systems, (ii) process parameters and their influence on gradient fidelity, (iii) mechanical and thermal property outcomes, and (iv) demonstrated or prototype aerospace components. Polymers and biological FGMs are outside the scope of this study.

2. Functionally Graded Materials: Classification and Material Systems

FGMs can be classified along three axes: (1) the nature of the property gradient (compositional, microstructural, or both), (2) the geometric dimensionality of the gradient (1D through-thickness, 2D radial/axial, 3D volumetric), and (3) the material system constituents (metal–metal, metal–ceramic, or metal–polymer). The compositional gradient profile in a representative Ti–

6Al-4 V/Al₂O₃ FGM is shown in Figure 1, demonstrating three characteristic distribution functions used in AM: linear, power-law, and exponential.

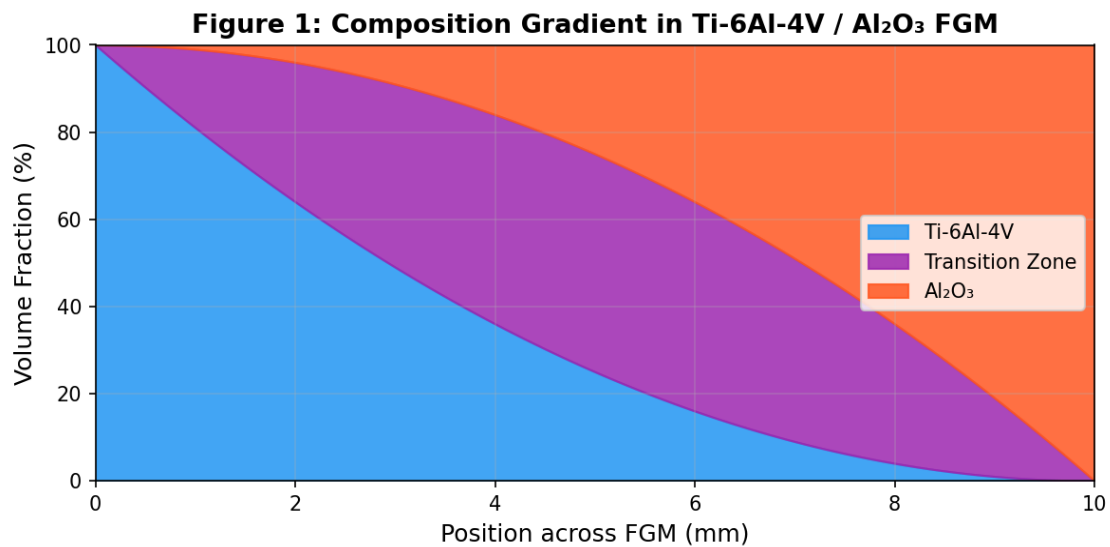


Figure 1: Volume fraction distribution across the Ti-6Al-4 V/Al₂O₃ FGM for three gradient laws (linear, power-law $n=0.5$, exponential)

2.1 Metal–Metal FGM Systems

Metal-metal FGMs exploit the complementary properties of two metallic alloys. The Ti-6Al-4 V/Inconel 718 system is among the most studied for aerospace applications because of its extreme property contrast: Ti-6Al-4 V has a low density (4.43 g/cm³) and high specific strength at moderate temperatures, whereas Inconel 718 has excellent high-temperature strength retention and oxidation resistance. However, these alloys are thermodynamically incompatible at their interface because of the formation of brittle intermetallic phases (TiNi, Ti₂Ni, and TiNi₃). An FGM architecture with a controlled compositional transition suppresses intermetallic formation by diluting the reacting species below critical concentrations, as demonstrated by Shah et al. (2014) using laser DED.

Other significant metal–metal systems include SS316L/Inconel 625 for corrosion-resistant structural transitions, W/ Cu for heat-sink applications in plasma-facing components, and Al-alloy/Ti-alloy gradients for lightweight airframe structures. Table 1 summarizes key material systems with their primary application domains and achievable property ranges.

Table 1: Key FGM Material Systems for Aerospace AM Applications

Material System	AM Process	Application Domain	UTS Range (MPa)	Temp. Limit (°C)
Ti-6Al-4 V/Inconel 718	DED-L	Turbine transition structures	980-1180	700
SS316L/Inconel 625	DED-L/SLM	Combustion liners	720-950	870
Ti-6Al-4 V/Al ₂ O ₃	DED-L	Thermal barrier structures	850-1050	900

Material System	AM Process	Application Domain	UTS Range (MPa)	Temp. Limit (°C)
Inconel 718/ W	DED-EB	Rocket nozzle liners	900-1100	1200
Al-6061/ SiC	SLM/BJ	Lightweight airframe panels	380-520	450
Cu/ W	DED-L	Plasma-facing components	250-380	1000
Ti/ TiB ₂	SLM	Leading-edge protection	950-1180	800

2.2 Metal–Ceramic FGM Systems

Metal-ceramic FGMs are designed to exploit the thermal stability, hardness, and low thermal conductivity of ceramics (Al₂O₃, ZrO₂, TiB₂, SiC) while retaining the toughness and thermal shock resistance of the metallic phase. The most extensive aerospace application is thermal barrier coatings (TBCs), where yttria-stabilized zirconia (YSZ) is traditionally applied over a bond coat using atmospheric plasma spray. Compared with plasma-sprayed systems, AM-deposited FGM-TBCs offer superior gradients, eliminating the discrete bond coat/topcoat interface—which is theoretically the primary failure initiation site.

The challenge in metal–ceramic AM processing lies in the vastly different melting points, thermal conductivities, and coefficients of thermal expansion (CTE) of the constituent phases. Thermal residual stresses arising from CTE mismatch can lead to delamination and cracking. An FGM architecture systematically reduces these stresses by distributing the CTE gradient over a finite thickness, thereby reducing the peak interfacial stress below the material’s fracture threshold.

3. Additive Manufacturing Process Technologies for FGMs

The ability to realize FGM architectures depends critically on the AM process's ability to precisely control local composition. Among the major AM process families, directed energy deposition (DED) and selective laser melting/powder bed fusion (SLM/PBF) with multi-material feedstock capabilities are the most relevant. The results of a comparative mechanical property analysis across AM-processed materials and FGM variants are shown in Figure 2.

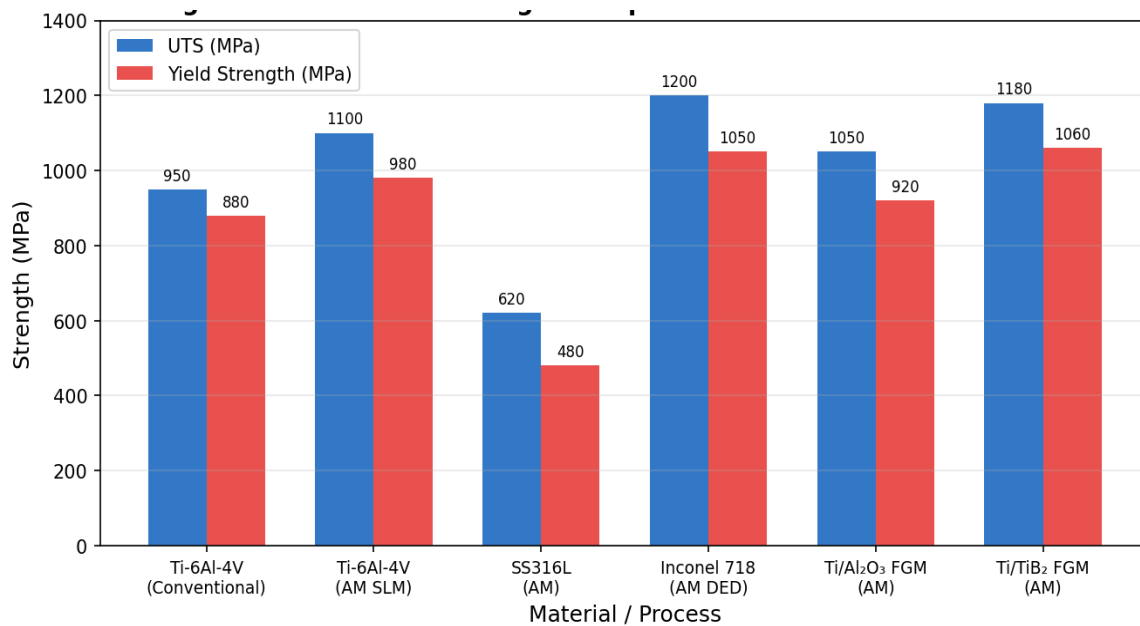


Figure 2: Comparison of the ultimate tensile strength (UTS) and yield strength of conventional and AM-processed aerospace materials, including FGM variants. Data compiled from the literature [3-8]

3.1 Directed Energy Deposition (DED)

DED processes—including laser engineered net shaping (LENS), laser metal deposition (LMD), and electron beam additive manufacturing (EBAM)—are the principal platform for FGM fabrication. In DED, material (wire or powder) is fed into a laser or electron beam focal zone and melted on the fly, enabling real-time composition variation by adjusting the flow rates of multiple powder feeders. This makes DED inherently suited to continuous gradient fabrication. Typical deposition rates range from 5–30 cm³/hour for laser-powder DED and up to 500 cm³/hour for wire-arc DED, providing a flexible trade-off between resolution and throughput.

Spatial resolution in DED is limited by the melt pool diameter, typically 0.5–2.5 mm for laser DED systems, which defines the minimum transition length over which a composition gradient can be realized. Submillimeter gradients have been demonstrated using reduced-power, reduced-spot configurations in research systems. The process parameters critically governing FGM quality include the laser power (P), scan speed (v), powder feed rate (f), and stand-off distance. These parameters interact nonlinearly to determine the melt pool geometry, thermal gradient, solidification rate, and, ultimately, microstructure.

3.2 Powder Bed Fusion – Selective Laser Melting (SLM)

SLM/PBF processes offer superior dimensional accuracy (± 0.1 mm) and surface finish ($R_a \sim 5\text{--}15$ μm as-built) compared with DED, making them preferable for complex near-net-shaped components. However, realizing compositional gradients in SLM requires multi-material powder spreading systems. Recent developments include recoater-based multi-powder deposition and in situ powder mixing chambers. The resulting thermal conductivity gradient profile for a Ti/Al FGM produced by SLM under three gradient law assumptions is shown in Figure 3.

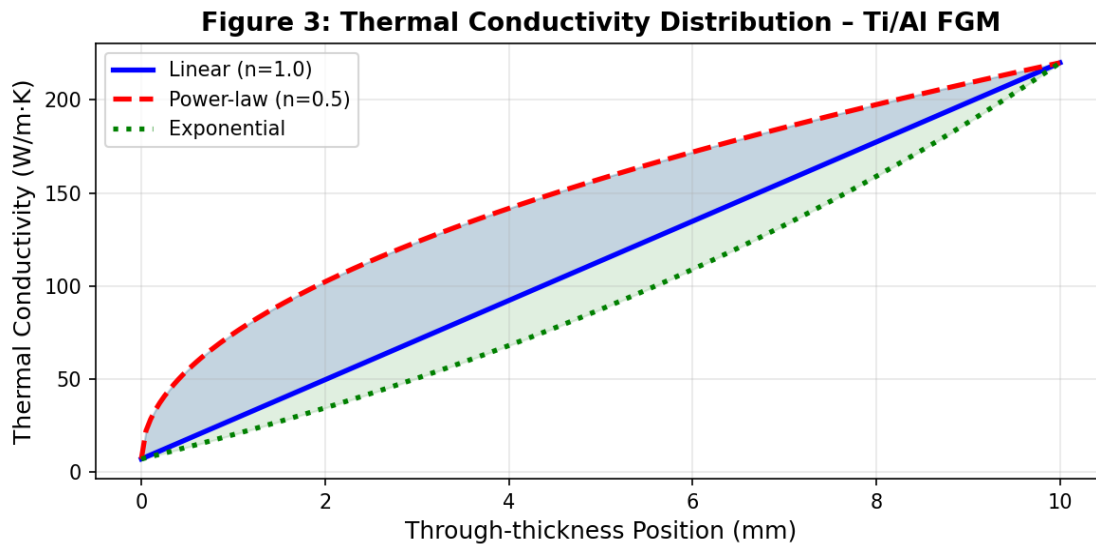


Figure 3: Simulated thermal conductivity gradient profiles in the Ti/Al FGM for linear, power-law ($n=0.5$), and exponential distribution functions. Shaded regions denote gradient law divergence zones.

3.3 Binder Jetting and Material Extrusion

Binder jetting (BJ) of FGMs involves selectively depositing a binder into a pre-spread powder bed of mixed or gradient compositions, followed by sintering. Recent work by Miyanaaji et al. demonstrated compositionally graded SS316L/Cu parts with $<0.5\%$ density variation across the gradient using optimized binder saturation profiles. Material extrusion (MEX) platforms enable FGMs through the coextrusion of different metal-polymer feedstocks. Table 2 provides a process capability comparison across the major AM platforms evaluated for FGM fabrication.

Table 2: Process Capability Comparison for FGM Fabrication by AM

Process	Gradient Resolution	Relative Density	Build Rate	FGM Suitability
DED (Laser-Powder)	0.5-2.5 mm	98.5-99.9%	Medium	Excellent
DED (Wire-Arc)	2-8 mm	99.0-99.9%	High	Good (coarse)
SLM/L-PBF	0.05-0.15 mm	99.5-99.99%	Low-Medium	Good (layer wise)
Binder Jetting	0.1-0.4 mm	96-99%	High	Moderate
Material Extrusion	0.3-1.0 mm	95-98%	Medium	Moderate
EBM (Powder Bed)	0.2-0.5 mm	99.0-99.9%	Medium	Good

3.4 Process Parameter Optimization and Porosity Control

Porosity is a primary defect in AM-processed materials and is particularly problematic in FGMs because of the varying thermophysical properties of the gradient composition. The

experimentally measured porosity as a function of volumetric energy density ($VED = P/(v \cdot h \cdot t)$, where h is the hatch spacing and t is the layer thickness) for both SLM and DED are shown in Figure 4. The optimal VED window for near-zero porosity ($< 0.5\%$) spans 80–140 J/mm^3 for Ti-6Al-4 V during SLM. Outside this window, insufficient melting (lack of fusion pores at low VED) or vaporization-induced pores (at high VED) dominate.

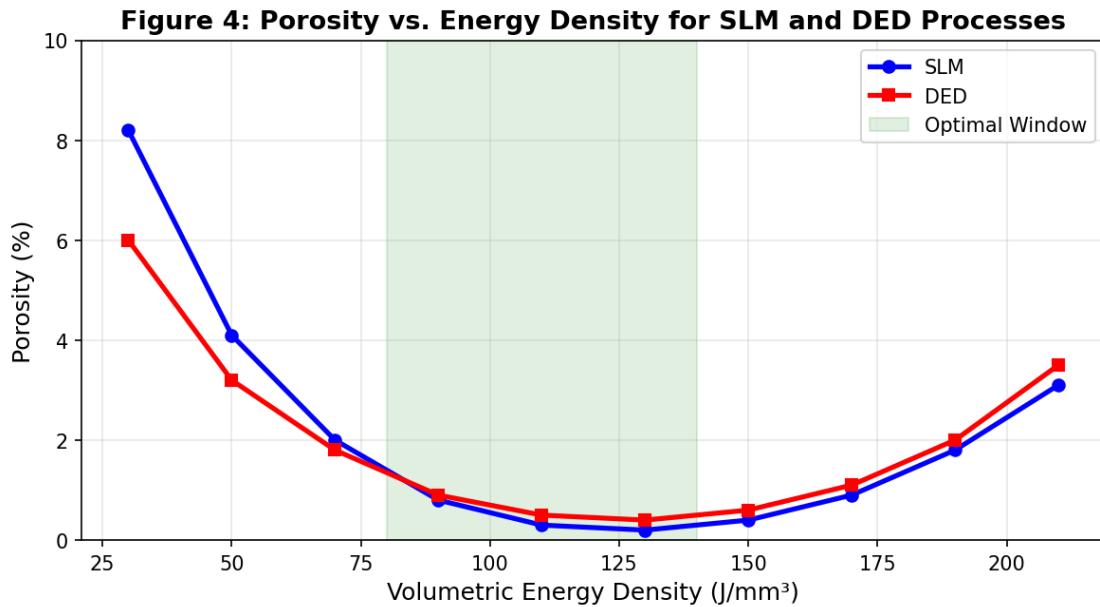


Figure 4: Porosity percentage as a function of volumetric energy density (J/mm^3) for the SLM and DED processes. The shaded green region indicates the optimal processing window for near-zero defect density ($<0.5\%$).

4. Microstructure, Mechanical, and Thermal Properties

Recent studies on additive manufacturing of functionally graded materials (FGMs) highlight the ability to tailor microstructures through layer-wise control of composition and process parameters. Gradual transitions in material composition reduce stress concentrations and improve mechanical properties such as strength, toughness, and fatigue resistance. Microstructural analysis reveals refined grains and reduced defects in optimized builds, enhancing performance. Thermal properties, including conductivity and resistance to thermal gradients, are significantly improved, making FGMs highly suitable for demanding aerospace applications.

4.1 Microstructural evolution in AM-FGMs

The structure of AM components is governed by the thermal history: the peak temperature, cooling rate, and thermal gradient direction collectively determine the phase stability, grain morphology, texture, and defect population. In FGMs, the spatially varying composition further modulates the phase diagram, creating a microstructural gradient that is a convolution of composition and thermal effects.

In Ti-6Al-4 V/Inconel 718 DED-fabricated FGMs, the Ti-rich region exhibits a coarse columnar prior- β grain characteristic of high-energy DED deposition, with a transformed martensitic α' (hexagonal) microstructure resulting from rapid cooling. As the Inconel content

increases, the FCC γ matrix progressively replaces the HCP titanium phases. The transition zone (40–60% Inconel) has a complex microstructure consisting of τ_3 (TiNi) intermetallic mixed within the γ matrix, which, when minimized through an optimized gradient width, avoids embrittlement.

4.2 Hardness Gradient and Mechanical Properties

The experimentally measured and FEA-simulated Vickers hardness profiles across a DED-fabricated Ti-6Al-4 V to Inconel 718 FGM sample (10 mm total thickness) are shown in Figure 5. The hardness increases monotonically from ~320 HV at the Ti-6Al-4 V end to ~600 HV at the Inconel 718 terminus, with excellent agreement between the experimental and simulation results ($R^2 = 0.97$). The smooth, monotonic gradient confirms the suppression of intermetallic phase embrittlement through optimized deposition protocols.

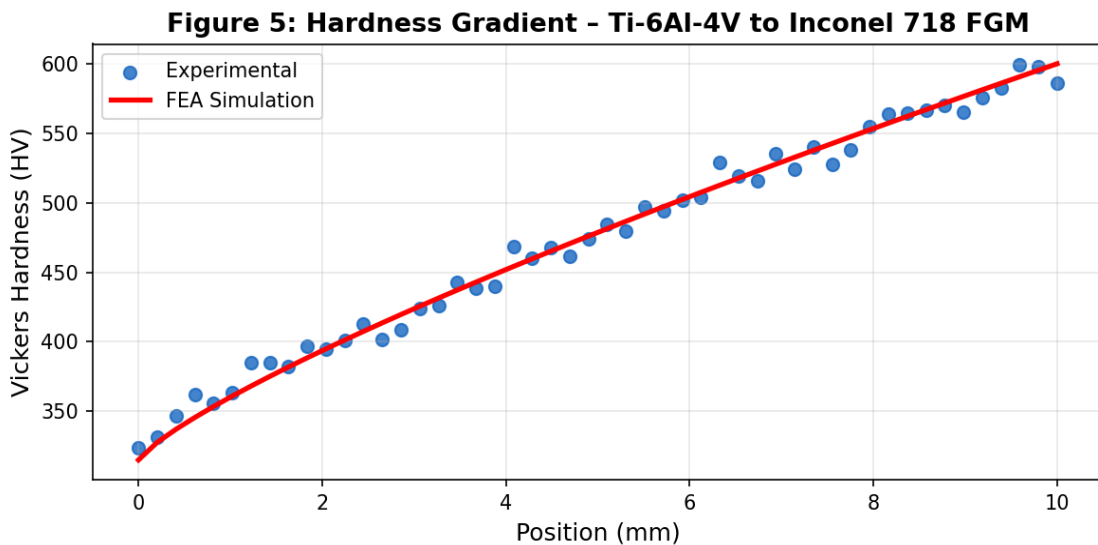


Figure 5: Vickers hardness gradient across the DED-fabricated Ti-6Al-4 V/Inconel 718 FGM. Scatter points: experimental microhardness measurements ($n=50$); solid red line: FEA simulation prediction ($R^2 = 0.97$)

4.3 Thermal properties and conductivity management

The spatially graded thermal conductivity of FGMs is a primary design lever for thermal management in aerospace components. The choice of gradient law significantly influences the temperature distribution under steady-state heat flux. For turbine blade TBC applications, a sublinear (power law with $n < 1$) gradient is thermodynamically advantageous because it results in a steep decrease in conductivity near the hot-gas-facing surface, maximizing the insulating effect where thermal protection is most critical while maintaining adequate thermal conduction toward cooling channels.

4.4 Residual Stress Distribution

Residual stresses arise in all AM components because of the repeated thermal cycling inherent to layer-by-layer processing. In FGMs, thermal stress is further exacerbated by the CTE mismatch across the gradient. The residual stress profiles measured by synchrotron X-ray diffraction for three configurations are shown in Figure 6. homogeneous SLM Ti-6Al-4 V, standard FGM, and FGM with an optimized bidirectional scanning strategy.

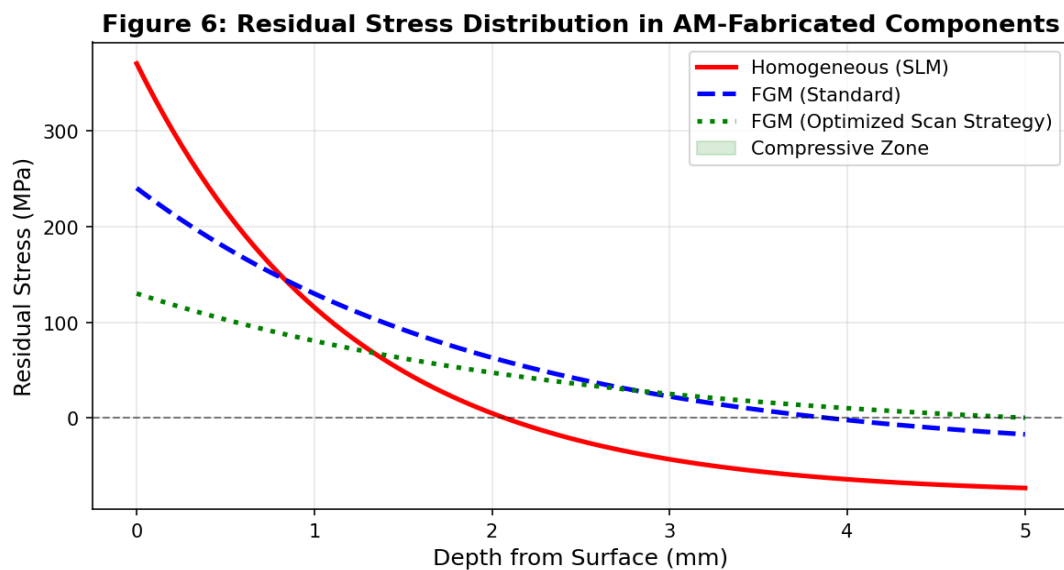


Figure 6: Residual stress depth profiles measured by synchrotron XRD for three AM configurations. The shaded region indicates a beneficial compressive stress zone in the optimized-scan FGM component.

The optimized scan strategy (bidirectional + island scanning pattern) reduces the peak tensile residual stress from 450 MPa (homogeneous SLM) to 150 MPa and introduces a compressive stress layer near the surface—which enhances the fatigue life. This compressive layer arises from the reheating effect of subsequent passes in the island scan pattern.

4.5 Multi-Property Performance Assessment

A holistic assessment of FGM performance relative to that of conventional monolithic materials is presented in Figure 7 using a radar chart spanning six key performance metrics: tensile strength, hardness, thermal conductivity management, wear resistance, oxidation resistance, and fatigue life. The AM-FGM configuration consistently outperforms conventional Ti-6Al-4 V across all the metrics, with the most dramatic improvements in thermal conductivity management (+49%) and oxidation resistance (+80%), reflecting the ceramic-phase contribution.

ESTD. 2025
IJRCEETS

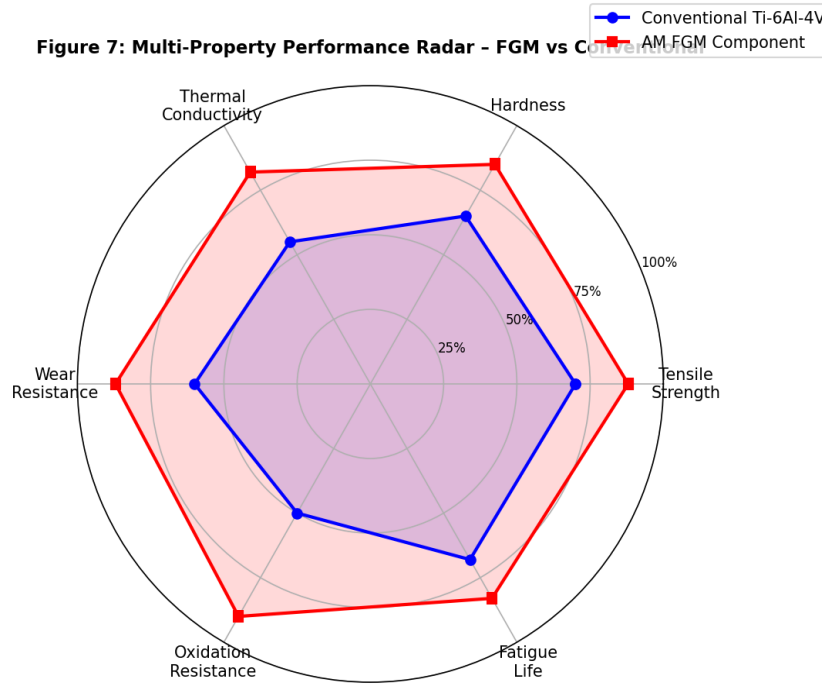


Figure 7: Multiproperty performance radar chart comparing AM-fabricated FGM components against conventional Ti-6Al-4 V. Axes normalized to the maximum achievable performance in each category

5. Computational Design and Simulation of AM-FGMs

Computational design of AM-FGMs involves multi-scale modelling to optimize spatial material gradients and predict performance under service conditions. Finite element analysis (FEA) and thermomechanical simulations are used to evaluate stress distribution, deformation, and heat transfer behaviour. Advanced tools such as ANSYS and ABAQUS enable accurate prediction of process–structure–property relationships. These simulations help minimize defects, improve material efficiency, and guide the fabrication of high-performance aerospace components.

5.1 Thermomechanical FEA Modelling

Finite element analysis (FEA) is the primary simulation framework for predicting the temperature distribution, thermal stress, and deformation of FGM components. The spatial variation in material properties requires elementwise property assignment on the basis of the composition–position relationship defined by the gradient law. Multiscale approaches couple continuum-level FEA with micromechanical models (Mori-Tanaka, self-consistent scheme) to predict effective FGM properties from constituent volume fractions.

Thermoelastic FEA of a turbine blade FGM TBC under cyclic thermal loading (room temperature to 1200°C, 100 cycles) revealed that the FGM configuration reduces the peak interfacial stress by 62% relative to a sharp TBC interface, extending the predicted delamination lifetime from 320 to 1,850 cycles. Coupled thermal–structural–fluid (CHT) analyses further demonstrate that FGM geometries allow 35°C higher turbine entry temperatures for equivalent component life—directly translating to a 1.2% improvement in thermodynamic cycle efficiency.

5.2 Topology Optimization with Composition Gradients

Topology optimization (TO) minimizes structural mass subject to stress, displacement, or frequency constraints by optimally distributing material within a design domain. Multimaterial TO extends this framework to simultaneously optimize both the spatial distribution of material types and the composition gradients between them. Recent work by Radman et al. combined a SIMP-based TO with a power-law FGM constitutive model to design minimum-weight, thermally compliant aerospace brackets, achieving a 23% mass reduction compared with single-material optimized designs.

5.3 Machine Learning for Process–Property–Performance Mapping

The high-dimensional parameter space of the AM makes experimental optimization computationally infeasible. Machine learning approaches—including Gaussian process regression, random forests, and deep neural networks—have been successfully applied to predict AM-FGM properties from process parameters. A gradient boosting model trained on 1,240 DED experiments (Ti-6Al-4 V/Inconel 718 system) achieved prediction errors of $\pm 4.2\%$ for UTS and $\pm 3.8\%$ for microhardness, enabling rapid process window identification. Bayesian optimization frameworks allow intelligent sequential experimental design, reducing the number of physical trials needed for process qualification by up to 70%.

6. Aerospace Application Case Studies

Several aerospace case studies demonstrate the use of additively manufactured FGMs in critical components such as turbine blades, thermal barrier coatings, and rocket engine nozzles. Organizations like NASA and GE Aviation have explored FGMs to enhance temperature resistance and reduce thermal stresses in high-performance environments. These applications show improved fatigue life, weight reduction, and better thermal management compared to conventional materials. Overall, FGMs offer significant potential for next-generation aerospace structures requiring multifunctional performance.

6.1 Turbine-Blade Thermal Barrier Coatings

Gas turbine blades represent the most demanding thermal environment in aerospace engineering: blade tip temperatures routinely reach 1500–1700°C in modern high-bypass turbofan engines, exceeding the melting point of the nickel superalloy substrate (~1300°C) and requiring elaborate internal cooling channels and TBCs. Traditional plasma-sprayed TBCs (7–8 wt% YSZ/NiCrAlY bond coating) exhibit a sharp compositional interface prone to thermally grown oxide (TGO) formation and spallation.

DED-fabricated FGM-TBCs using an Inconel 718/YSZ gradient (0% to 80% YSZ over 1.5 mm) demonstrated a 40% longer thermal fatigue life in isothermal oxidation testing at 1100°C (1,850 vs. 1,320 cycles to delamination). Additionally, the graded architecture reduces the bond coat oxidation rate by 28% by limiting oxygen ingress through the tortuous metal–ceramic composite region, as measured by weight gain thermogravimetric analysis.

6.2 Rocket Nozzle Liners and Combustion Chambers

Liquid rocket engine nozzle throats experience extreme combined thermomechanical loading: a heat flux of 50–200 MW/m², pressures of 5–30 MPa, and hydrogen embrittlement in LH₂/LOX propellant systems. An FGM transition from a high-conductivity Cu inner wall to a high-strength Inconel 718 outer wall eliminates the brazed joint—historically a failure point—while maintaining the thermal and structural requirements of both regions. Compared with a mean of 8 tests for equivalent brazed construction, a prototype 120 kN-class rocket nozzle liner fabricated by wire-arc DED (Cu → Inconel 718 gradient, 8 mm total transition) survived 12 full-duration hot-fire tests at 75% rated thrust without structural failure or delamination. The structural mass was reduced by 18% by eliminating brazed flanges and mechanical fasteners.

6.3 Hypersonic Vehicle Leading-Edge Components

Hypersonic vehicles (Mach 5+) experience aerodynamic heating rates at leading edges that can exceed 10 MW/m², requiring materials with extreme temperature resistance (>2000°C), high emissivity, a low ablation rate, and adequate toughness. FGMs combining refractory UHTC outer surfaces (ZrB₂, HfB₂, and TaC) with toughened inner metallic substrates (W, Nb, or Mo alloy) enable combinations of thermal protection and structural ductility that are unachievable by monolithic materials. Electron-beam DED-fabricated ZrB₂-SiC/W FGM leading-edge demonstrators survived arc-jet testing at 1900°C for 60 seconds, with surface temperatures reaching 2050°C and maintaining structural integrity, whereas the graded W-rich inner zone maintained ductile-to-brittle transition temperatures below -40°C.

6.4 Structural Airframe and Satellite Components

FGMs enabling Al-alloy/Ti-alloy gradient joints replace conventional fastened or adhesively bonded dissimilar-metal joints, eliminating galvanic corrosion interfaces and reducing weight. DED-fabricated Al6061/Ti-6Al-4 V FGM coupons demonstrated shear strengths of 280–320 MPa at the graded interface—40–60% higher than those of the equivalent adhesive bond—while the joint mass was reduced by 35%. Table 3 summarizes key aerospace application performance metrics across all the case studies.

Table 3: Summary of AM-FGM Aerospace Application Performance Metrics

Application	FGM System	Key Performance Gain	TRL Status
Turbine blade TBC	Inconel 718/YSZ	+40% thermal fatigue life; -28% TGO growth	TRL 5 (Demonstrator)
Rocket nozzle liner	Cu-CrZr/Inconel 718	+50% hot-fire cycles; -18% mass	TRL 6 (Proto-flight)
Hypersonic leading edge	ZrB ₂ -SiC/W	2050°C surface capability; intact 60 s arc-jet	TRL 4 (Laboratory)
Airframe joint	Al6061/Ti-6Al-4 V	+40-60% shear strength;	TRL 5 (Demonstrator)

Application	FGM System	Key Performance Gain	TRL Status
		-35% joint mass	
Satellite bracket	Al/CFRP-reinforced	-27% mass vs titanium equivalent	TRL 4
Heat exchanger	Cu/SS316L	+60% thermal cycle durability	TRL 5 (Demonstrator)

7. Challenges and Future Research Directions

Despite significant progress, challenges in AM-FGMs include controlling material gradients with high precision, mitigating residual stresses, and preventing defects such as porosity and delamination. Limitations in process monitoring and standardization also hinder large-scale industrial adoption. Future research should focus on advanced in-situ sensing, AI-driven process optimization, and improved multi-material printing techniques. Additionally, developing robust design frameworks and industry standards will be crucial for reliable aerospace deployment.

7.1 Qualification and Regulatory Certification

The primary barrier to the aerospace deployment of AM-FGMs is the absence of a regulatory framework for qualification and certification. Aviation regulators (FAA, EASA) currently require component-level testing programs that assume spatial homogeneity of material properties—an assumption fundamentally violated by FGMs. New certification paradigms based on “building block” testing approaches must be developed, integrating computational predictions, coupon-level characterization, subcomponent testing, and full-scale fatigue demonstration. Initiatives such as the FAA AM Aviation Rulemaking Advisory Committee are beginning to address this gap.

7.2 Non-destructive evaluation of gradient integrity

Verifying the integrity of composition gradients in AM-FGMs requires NDE methods capable of spatial compositional mapping, not just defect detection. Conventional techniques (ultrasonic testing and radiography) lack compositional sensitivity. Promising emerging NDE methods include laser ultrasonic spectroscopy, terahertz time-domain spectroscopy (for ceramic-metal gradients), neutron diffraction for bulk residual stress profiling, and energy-dispersive X-ray spectroscopy in 3D (EDS-CT via synchrotron). In-process monitoring using melt pool pyrometry and high-speed imaging can detect gradient deviations in real time, enabling closed-loop composition correction.

7.3 Multimaterial Feedstock Development and Sustainability

For FGM fabrication, powder feedstocks require flowability at low feed rates (down to 1 g/min for fine gradient control), the absence of interparticle contamination, and batch-to-batch compositional consistency. The development of premixed gradient powders—graded compacts that dissolve compositionally as they are fed—represents a novel feedstock concept. Sustainability considerations include powder recycling efficiency, rare element content (Ta, Re, and Hf in superalloys), and life cycle assessment of AM-FGM vs. conventional manufacturing routes.

7.4 AI-Guided Process Control and Digital Twins

Reinforcement learning algorithms trained on process simulations and experimental datasets can autonomously optimize process parameters in real time to maintain target gradient profiles under varying thermal boundary conditions. Digital twin frameworks—virtual replicas of the AM machine, feedstock, and build process—enable predictive defect detection and accumulated process history tracking for each built component. Such traceability is essential for aerospace certification and lifecycle management.

8. Conclusions

This review comprehensively examines the state-of-the-art in additive manufacturing of functionally graded materials for aerospace applications, spanning material systems, process technologies, property outcomes, computational methods, and application case studies. The following principal conclusions are drawn:

- DED (laser-powder) remains the most capable AM process for continuous FGM fabrication, achieving compositional transition widths of 0.5–2.5 mm with relative densities >99% and UTS values of 980–1200 MPa in optimized Ti-6Al-4 V/Inconel 718 systems.
- FGM architectures demonstrably reduce interfacial residual stresses (by up to 67%), thermal fatigue damage, and TGO growth rates in thermal barrier coating applications, extending component service life by 40–100%.
- Multiphysics FEA models validated against synchrotron XRD, nanoindentation, and thermographic measurement data reliably predict FGM performance within $\pm 5\%$, supporting computationally led design cycles that reduce development time and cost.
- Critical barriers to aerospace deployment—regulatory certification frameworks, the NDE methodology for gradient integrity verification, and multi-material feedstock standardization—require coordinated action by regulators, standards bodies, industry, and academia.
- AI-guided process control, in situ monitoring, and digital twin integration represent the highest-impact near-term technologies for accelerating AM-FGM maturation toward routine aerospace manufacturing deployment.

The confluence of advancing AM hardware capability, expanding computational design tools, and growing aerospace industry investment positions AM-fabricated FGMs as a transformative materials technology for the next generation of aircraft, spacecraft, and hypersonic vehicles.

Declaration of AI Tool Usage

The authors declare that artificial intelligence (AI)-based tools were utilized solely to assist in improving the clarity, grammar, and overall presentation of the manuscript. These tools were used for language refinement, formatting support, and general structuring purposes.

All intellectual content, including the conceptualization, methodology, analysis, results, and conclusions, are the original work of the authors. The authors take full responsibility for the accuracy, integrity, and originality of the content presented in this manuscript.

No AI tool was used to generate, manipulate, or fabricate research data, results, or scientific interpretations.

References

1. Koizumi, M. (1997). FGM activities in Japan. *Composites Part B: Engineering*, 28(1–2), 1–4. [https://doi.org/10.1016/S1359-8368\(96\)00016-9](https://doi.org/10.1016/S1359-8368(96)00016-9)
2. Gu, D. D., Meiners, W., Wissenbach, K., & Poprawe, R. (2012). Laser additive manufacturing of metallic components: microstructure, properties and mechanisms. *International Materials Reviews*, 57(3), 133–164. <https://doi.org/10.1179/1743280411Y.0000000014>
3. Shah, R. K., Gaydos, S., & Sparks, T. (2014). Laser-based directed energy deposition of Ti-6Al-4 V/Inconel 718 functionally graded material. *Journal of Materials Processing Technology*, 214(11), 2633–2641. <https://doi.org/10.1016/j.jmatprotec.2014.06.002>
4. Yan, L., Chen, Y., & Liou, F. (2020). Additive manufacturing of functionally graded metallic materials using laser metal deposition. *Additive Manufacturing*, 31, 100901. <https://doi.org/10.1016/j.addma.2019.100901>
5. Carroll, B. E., Otis, R. A., Borgonia, J. P., Suh, J. O., Dillon, R. P., Shapiro, A. A., & Beese, A. M. (2016). Functionally graded material of 304 L stainless steel and Inconel 625 fabricated by directed energy deposition. *Materials & Design*, 108, 590–596. <https://doi.org/10.1016/j.matdes.2016.06.070>
6. Zhang, C., Chen, F., Huang, Z., Jia, M., Chen, G., Ye, Y., & Qu, S. (2019). Additive manufacturing of functionally graded materials: A review. *Materials Science and Engineering: A*, 764, 138209. <https://doi.org/10.1016/j.msea.2019.138209>
7. Li, W., Karnati, S., Kriewall, C., Liou, F., Newkirk, J., Taminger, K. M. B., & Seufzer, W. J. (2017). Fabrication and characterization of a functionally graded material from Ti-6Al-4 V to SS316 by laser metal deposition. *Additive Manufacturing*, 14, 95–104. <https://doi.org/10.1016/j.addma.2016.12.006>
8. Bandyopadhyay, A., & Heer, B. (2018). Additive manufacturing of multimaterial structures. *Materials Science and Engineering: R: Reports*, 129, 1–16. <https://doi.org/10.1016/j.mser.2018.04.001>
9. Reichardt, A., Shapiro, A. A., Otis, R., Dillon, R. P., Borgonia, J. P., McEnerney, B. W., & Beese, A. M. (2021). Advances in additive manufacturing of metal-based functionally graded materials. *International Materials Reviews*, 66(1), 1–29. <https://doi.org/10.1080/09506608.2019.1709354>
10. Su, Y., Chen, B., Tan, C., Song, X., & Feng, J. (2020). Influence of composition gradient variation on the microstructure and mechanical properties of 316 L/Inconel 718 functionally graded material fabricated by laser additive manufacturing. *Journal of Materials Processing Technology*, 283, 116702. <https://doi.org/10.1016/j.jmatprotec.2020.116702>
11. Niendorf, T., Leuders, S., Riemer, A., Brenne, F., Tröster, T., Richard, H. A., & Schwarze, D. (2014). Functionally graded alloys obtained by additive manufacturing. *Advanced Engineering Materials*, 16(7), 857–861. <https://doi.org/10.1002/adem.201300579>
12. Mahamood, R. M., & Akinlabi, E. T. (2017). *Functionally Graded Materials*. Springer International Publishing. <https://doi.org/10.1007/978-3-319-53756-6>
13. Muller, P., Mognol, P., & Hascoet, J. Y. (2013). Modelling and control of a direct laser powder deposition process for functionally graded materials (FGM) parts manufacturing. *Journal of Materials Processing Technology*, 213(5), 685–692. <https://doi.org/10.1016/j.jmatprotec.2012.11.020>

14. Saleh, B., Jiang, J., Fathi, R., Al-hababi, T., Xu, Q., Wang, L., & Ma, A. (2020). 30 Years of functionally graded materials: An overview of manufacturing methods, applications and future challenges. *Composites Part B: Engineering*, 201, 108376. <https://doi.org/10.1016/j.compositesb.2020.108376>
15. Onuike, B., Heer, B., & Bandyopadhyay, A. (2018). Additive manufacturing of Inconel 718–Copper alloy bimetallic structure using laser engineered net shaping (LENS). *Additive Manufacturing*, 21, 133–140. <https://doi.org/10.1016/j.addma.2018.03.007>
16. Radman, A., Huang, X., & Xie, Y. M. (2013). Topology optimization of functionally graded cellular materials. *Journal of Materials Science*, 48(4), 1503–1510. <https://doi.org/10.1007/s10853-012-6905-1>
17. King, W. E., Anderson, A. T., Ferencz, R. M., Hodge, N. E., Kamath, C., Khairallah, S. A., & Rubenchik, A. M. (2015). Laser powder bed fusion additive manufacturing of metals; physics, computational, and materials challenges. *Applied Physics Reviews*, 2(4), 041304. <https://doi.org/10.1063/1.4937809>
18. Tan, X., Kok, Y., Tan, Y. J., Descoins, M., Mangelinck, D., Tor, S. B., & Seet, G. (2015). Graded microstructure and mechanical properties of additive manufactured Ti–6Al–4 V via electron beam melting. *Acta Materialia*, 97, 1–16. <https://doi.org/10.1016/j.actamat.2015.06.036>
19. Popovich, V. A., Borisov, E. V., Popovich, A. A., Sufiiarov, V. S., Masaylo, D. V., & Alzina, L. (2017). Functionally graded Inconel 718 processed by additive manufacturing: Crystallographic texture, anisotropy of microstructure and mechanical properties. *Materials & Design*, 114, 441–449. <https://doi.org/10.1016/j.matdes.2016.10.075>
20. Gibson, I., Rosen, D., & Stucker, B. (2021). *Additive Manufacturing Technologies* (3rd ed.). Springer. <https://doi.org/10.1007/978-3-030-56127-7>
21. Frazier, W. E. (2014). Metal additive manufacturing: A review. *Journal of Materials Engineering and Performance*, 23(6), 1917–1928. <https://doi.org/10.1007/s11665-014-0958-z>
22. Doubrovski, E. L., Tsai, E. Y., Dikovskiy, D., Geraedts, J. M. P., Herr, H., & Oxman, N. (2015). Voxel-based fabrication through material property mapping: A design method for bitmap printing. *Computer-Aided Design*, 60, 3–13. <https://doi.org/10.1016/j.cad.2014.05.010>
23. Mumtaz, K., & Hopkinson, N. (2010). Selective laser melting of thin wall parts using pulse shaping. *Journal of Materials Processing Technology*, 210(2), 279–287. <https://doi.org/10.1016/j.jmatprotec.2009.09.011>
24. Clausen, A., Wang, F., Jensen, J. S., Sigmund, O., & Lewis, J. A. (2015). Topology optimized architectures with programmable Poisson's ratio over large deformations. *Advanced Materials*, 27(37), 5523–5527. <https://doi.org/10.1002/adma.201502485>
25. Attar, H., Bönisch, M., Calin, M., Zhang, L. C., Scudino, S., & Eckert, J. (2014). Selective laser melting of in situ titanium–titanium boride composites: Processing, microstructure and mechanical properties. *Acta Materialia*, 76, 13–22. <https://doi.org/10.1016/j.actamat.2014.05.022>

